Microsc. Microanal. 16, 561–568, 2010
doi:10.1017/S1431927610093785

Microscopy AND Microanalysis

Dilution and Magnification Effects on Image Analysis Applications in Activated Sludge Characterization

D.P. Mesquita,[1] O. Dias,[1] R.A.V. Elias,[2] A.L. Amaral,[1,3] and E.C. Ferreira[1,*]

[1]*IBB—Institute for Biotechnology and Bioengineering, Centre of Biological Engineering, Universidade do Minho, Campus de Gualtar, 4710-057, Braga, Portugal*
[2]*Escola Superior de Tecnologia e de Gestão, Instituto Politécnico de Bragança, Campus de Santa Apolónia, Apartado 134, 5301-857 Bragança, Portugal*
[3]*Instituto Superior de Engenharia de Coimbra, Instituto Politécnico de Coimbra, Rua Pedro Nunes, Quinta da Nora, 3030-199 Coimbra, Portugal*

Abstract: The properties of activated sludge systems can be characterized using image analysis procedures. When these systems operate with high biomass content, accurate sludge characterization requires samples to be diluted. Selection of the best image acquisition magnification is directly related to the amount of biomass screened. The aim of the present study was to survey the effects of dilution and magnification on the assessment of aggregated and filamentous bacterial content and structure using image analysis procedures. Assessments of biomass content and structure were affected by dilutions. Therefore, the correct operating dilution requires careful consideration. Moreover, the acquisition methodology comprising a 100× magnification allowed data on aggregated and filamentous biomass to be determined and smaller aggregates to be identified and characterized, without affecting the accuracy of lower magnifications regarding biomass representativeness.

Key words: activated sludge, image analysis, dilution, magnification, aggregates, filaments

Introduction

Wastewater treatment plants (WWTP) are frequently operated with activated sludge systems, consisting of an aerated tank for aerobic sludge treatment and a clarifier for the settling stage to allow aggregated biomass to separate. An adequate balance between the different types of bacteria is essential for the formation of aggregates with acceptable properties of structure, stability, size and density. This results in effective settling of the sludge and low suspended solid effluent levels (Jenkins et al., 2003; Jin et al., 2003; Wilén et al., 2008). Recently, owing to advances in imaging hardware, automated image analysis methodologies have been increasingly adopted to monitor activated sludge properties. Activated sludge processes are currently monitored via microscopic observation for (a) determination of aggregated and filamentous bacterial content (da Motta et al., 2001; Cenens et al., 2002; Amaral, 2003; Banadda et al., 2005; Jenné et al., 2006, 2007), (b) prediction of settling ability based on image analysis and multivariate statistical techniques (Amaral & Ferreira, 2005; Mesquita et al., 2009*a*), and (c) protozoan and metazoan identification (Ginoris et al., 2007*a*, 2007*b*; Amaral et al., 2008). The fact that a number of activated sludge systems operate with high biomass contents suggests that during image acquisition samples should be diluted for adequate sludge characterization. When samples are not diluted, aggregates and filaments may appear super-imposed on images, which can be misleading (da Motta et al., 2002). Therefore, dilutions aid microscopic inspection of sludge, and when using image analysis methodologies they allow the system to be evaluated accurately. However, dilution techniques can be problematic as the amount of screened biomass decreases and they could lead to morphological changes of the aggregated biomass.

The majority of studies rely on image acquisition procedures and on microscopic visualization at 100× magnification (Abreu et al., 2007; Costa et al., 2007; Mesquita et al., 2009*a*, 2009*b*, 2010). The advantage of this methodology is that it allows aggregated and filamentous bacterial content and morphological data to be determined from the same image. However, the relationship between the image analysis data acquired at 100× magnifications and at a lower and more representative magnification should be investigated.

The present study describes the use of an image analysis procedure, developed for characterizing activated sludge systems using bright-field microscopy to investigate the effect of five different dilutions and two magnifications on image analysis data.

Received February 26, 2010; accepted June 2, 2010
*Corresponding author. E-mail: ecferreira@deb.uminho.pt

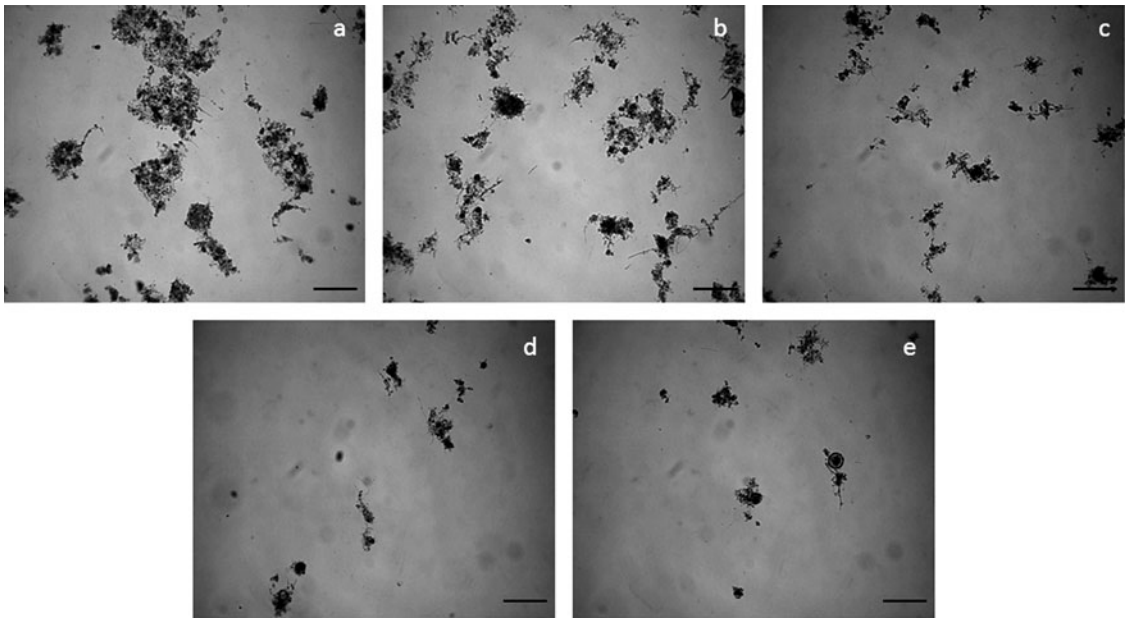

Figure 1. (**a**) Undiluted sample, (**b**) dilution 1:2, (**c**) dilution 1:5, (**d**) dilution 1:8, and (**e**) dilution 1:10. The scale bar represents 200 μm.

Material and Methods

For the dilution study, three samples were collected from an aeration tank in the municipal WWTP located in Braga (Portugal) treating domestic effluents. Total suspended solids (TSS) were determined by weight and the samples were within normal operating TSS values (4,708, 3,000, and 2,310 mg/L). For each sample, five dilutions were prepared: one part sludge to one, four, seven and nine parts water. To investigate the magnification effect (20× and 100×), a total of 13 samples were taken from two aerated basins of a WWTP treating domestic effluents, located in Bragança (Portugal). The contents and morphology of microbial aggregates and protruding filamentous bacteria were studied by bright-field image acquisition and analysis.

Image Acquisition

A volume of 25 μL was placed on a slide and covered with a 20 × 20 mm cover slip for visualization and image acquisition using bright-field microscopy. A recalibrated micropipette with a sectioned tip at the end, with a large enough diameter to allow larger aggregates to flow, was used to deposit samples on the slides. For dilution analysis, 200 images per sample (divided between three slides) were acquired in order to obtain significant data for all dilutions studied. Images were visualized using a Leitz Laborlux S optical microscope (Leitz, Wetzlar, Germany) with 100× total magnification, and acquired using a Zeiss AxioCam (Zeiss, Oberkochen, Germany) digital camera. Images were acquired using 1300 × 1030 pixels and an 8-bit format through the commercial software Axio Vision 3.1 (Zeiss). Approximately 25 images per sample were acquired for each magnification. The images were acquired with a NIKON SMZ 800–DIA stereomicroscope (Nikon, Tokyo) for the 20× total magnification (1× magnification apochromatic objective and 2× zoom factor), and with a NIKON NIK 50i CC/CF optic microscope (Nikon, Tokyo) for the 100× total magnification (10× magnification apochromatic objective). Images were acquired using a NIKON DS-5M-U1 (Nikon, Tokyo) digital camera with 1280 × 960 pixels and an 8-bit format through the commercial software NIS-ELEMENTS D (Nikon, Tokyo). Images of each dilution studied are presented in Figure 1.

Image Processing and Analysis

Aggregated and filamentous bacteria content and morphological descriptors were determined using image processing and analysis programs, adapted from Amaral and Ferreira (2005) in Matlab 7.3 language (The Mathworks, Inc., Natick, MA, USA). An image processing routine was used to obtain and save binary images of aggregated and protruding filamentous biomass. An image analysis program determined aggregate and filament content and morphological parameters. The image processing program comprises three stages: image pretreatment; segmentation; and debris elimination. The image analysis program determines morphological parameters. Figure 2 presents an example of original and binary images concerning the recognition of aggregated biomass (100× and 20× magnification) and filamentous bacteria (100× magnification).

The same image processing program was used for both magnifications, but no filamentous bacteria could be iden-

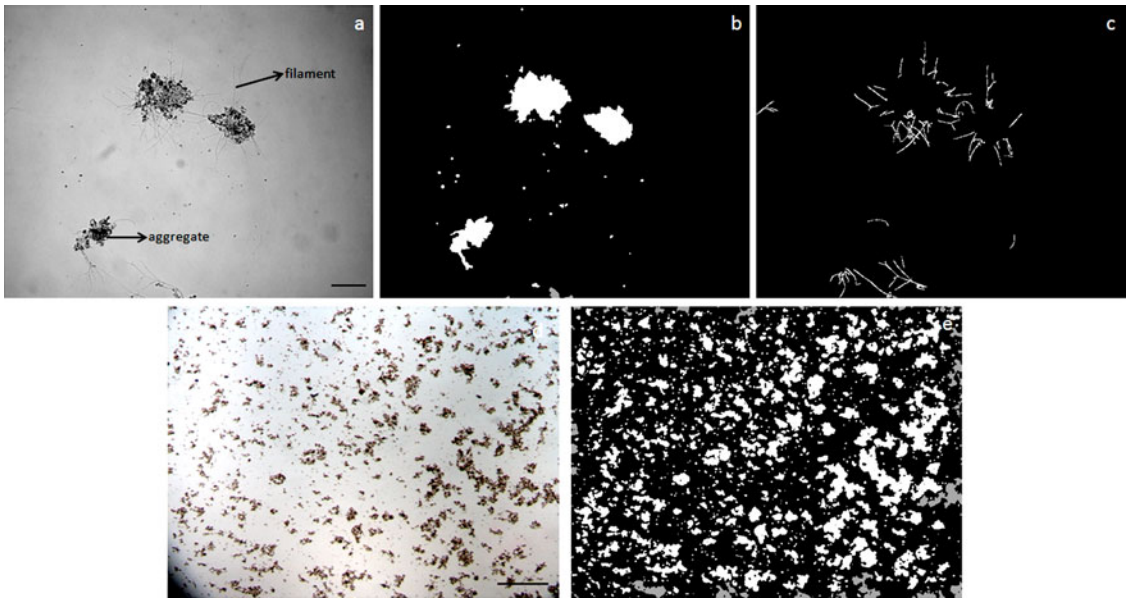

Figure 2. (**a**) Original image at 100× magnification (scale bar represents 200 μm), (**b**) binary image of aggregates, (**c**) binary image of filaments, (**d**) original image at 20× magnification (scale bar represents 50 μm), and (**e**) binary image of aggregates.

tified owing to their small size in the 20× magnification images.

Morphological Parameters

Characterization of activated sludge systems in terms of filamentous and aggregated biomass content and morphology can be obtained using image analysis methodologies (Amaral & Ferreira, 2005). For the dilution study, the area (*Area*) of each recognized aggregate (aggregate not bisected by the image boundaries) was calculated as the projected surface of the aggregate, whereas the total area of recognized aggregates per unit volume (TRA/Vol) was calculated as the sum of recognized aggregate areas per unit volume. Total filament content per unit volume (TL/Vol) was calculated as the total length of the filaments per unit volume, and the number of recognized aggregates per unit volume (Number/Vol) was calculated as the total number of recognized aggregates per unit volume (Amaral, 2003). Total filament content per total area of recognized aggregates (TL/TRA ratio) was obtained by dividing the TL/Vol by the TRA/Vol parameter. Equivalent diameter (D_{eq}) was calculated on the basis of the *Area* parameter using the following equation:

$$D_{eq} = 2F_{Cal}\sqrt{\frac{Area}{\pi}}, \quad (1)$$

where F_{Cal} is the calibration factor (μm per pixel).

Furthermore, aggregates were classified according to size in order to understand the dilution effect on biomass structure: small aggregates ($D_{eq} < 0.025$ mm), intermediate aggregates (0.025 mm $< D_{eq} <$ 0.25 mm), and large aggregates ($D_{eq} > 0.25$ mm). This classification has been used previously (Mesquita et al., 2009*a*, 2009*b*). For each class, recognized aggregates area percentage (Area %) was calculated as the ratio between the sum of each recognized aggregate area belonging to that class and the sum of the overall recognized aggregate areas. The aggregates recognition percentage parameter (Recognition %) was calculated as the ratio between the total recognized aggregates area and the total aggregates area (including aggregates bisected by the image boundaries).

Several parameters were used to investigate the relationship between the magnifications used in this study: total recognized aggregates area per volume (TRA/Vol); number of recognized aggregates per image (Number/Image); percentage number of recognized aggregates (Number %), calculated as the ratio between the total number of recognized aggregates in a class and the total number of recognized aggregates; recognized aggregates area percentage (Area %).

Statistical Analysis

For dilution analysis, a *runs test* was applied (Bradley, 1968) to image analysis data to calculate the number of different runs, the length of the runs and the *z*-value. An α-value of 0.05 (95% confidence) was used, and the *z*-value was compared with the Critical *z*-value for that α-value (1.96). For a *z*-value $<$ 1.96, the data exhibited random behavior, and for a *z*-value $>$ 1.96, they exhibited nonrandom behavior.

To compare the 20× and 100× acquisition methodologies, the two-sample *t*-test for averages was applied to the

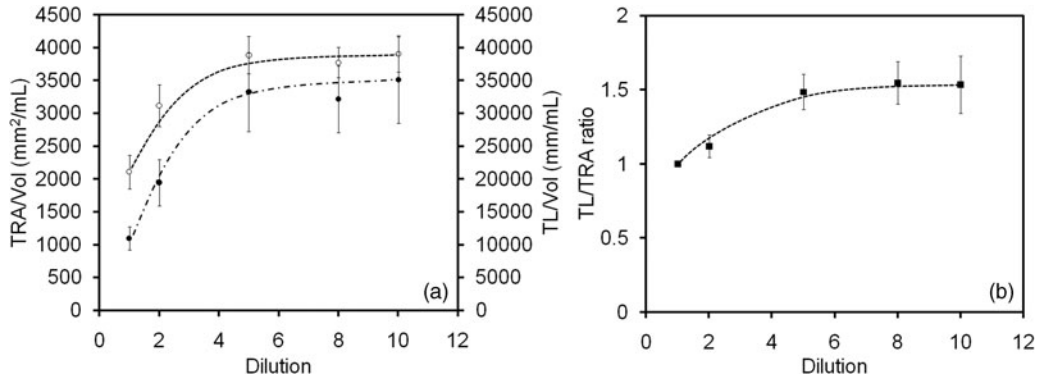

Figure 3. (**a**) Average values of the three samples for the five dilutions regarding TL/Vol (●), TRA/Vol (○), and (**b**) TL/TRA ratio (■).

image analysis data to calculate the Critical *t*-value, *t*-, and *p*-value. The number of observations was equal to the number of samples studied (13), and an α-value of 0.05 (95% confidence) was used. *t*- and *p*-values were compared with the Critical *t*-value and α-values. For $t <$ Critical *t*-value and $p > \alpha$, the averages of both methods were equal.

Results and Discussion

Dilution Study

When a dilution is performed the amount of screened biomass decreases, which can lead to incorrect characterization of the biomass within the biological system (da Motta et al., 2002). Furthermore, modification of the osmotic pressure when a dilution is performed can trigger biomass to deflocculate, causing subsequent release of floc-forming and filamentous bacteria to the mixed liquor, which can change the aggregate size and morphology. Therefore, precautions must be taken when diluting samples. However, dilutions could be advantageous in high biomass content systems, as smaller aggregates and protruding filaments can be hidden by larger aggregates in nondiluted samples. As presented in Figure 1, increasing dilutions caused aggregates to be more spaced out, allowing smaller aggregates and filamentous bacteria hidden by larger aggregates in undiluted samples to be identified. However, increasing dilutions led to a decrease of the screened biomass in each field of view and hindered the representativeness of each sample. The TL/Vol, TRA/Vol, and TL/TRA parameters, presented in Figure 3, were used to assess the dilution effect on activated sludge within normal operating TSS values (ranging from 2,310 to 4,708 mg/L).

The results depicted in Figure 3a demonstrate that TRA/Vol and TL/Vol converged to an asymptotic value after the fivefold (1:5) dilution. Both parameters were strongly influenced by dilution, increasing from the nondiluted sample to the fivefold dilution (run of three consecutive ascending values in both cases), probably due to the release of enclosed filamentous bacteria and aggregates, and biomass deflocculation phenomena. The TRA/Vol almost doubled (1.84 times) its nondiluted value when the fivefold dilution was performed, while TL/Vol increased 3.03 times for the same dilution. Therefore, it could be concluded that, despite the TRA and TL parameters converging to an asymptotic value after the fivefold dilution, TL was more affected by dilution than TRA. Considering the trend lines for TL and TRA, there is a correlation between the two parameters when increasing dilutions are performed (TL/TRA ratio dependence with dilution; see Fig. 3b). A well-defined trend line was obtained modeling the dependence of TL/TRA ratio on dilution, and as expected from the previous results, a threshold value (around 1.5) was obtained for the fivefold dilution. These results suggest that for the present study an optimal dilution (fivefold) was determined. This fivefold dilution unveiled all enclosed filamentous bacteria and aggregates, as verified by the absence of further increase in TRA and TL parameters. In the above cases, no z-values from the runs test were obtained to verify data randomness because there were too few data points (fewer than five) in each situation (below and above the fivefold dilution).

As discussed by da Motta et al. (2002), dilutions are related to assessment of the size and number of aggregates by image analysis techniques. This dependence on dilutions was evaluated by assessing the behavior of each aggregates class (smaller, intermediate, and larger) after dilution. Number/Vol, TRA/Vol, Area %, and equivalent diameter for each class of samples are depicted in Figures 4a, 4b, 4c, and 4d, respectively.

The results depicted in Figure 4a revealed a stabilization of the number of larger aggregates after a twofold dilution, following a small initial increase (from 264 to 496 aggregates/mL). This stabilization may suggest that no significant deflocculation took place for larger aggregates because their number did not decrease markedly with dilutions. However, analysis of the TRA/Vol behavior for larger aggre-

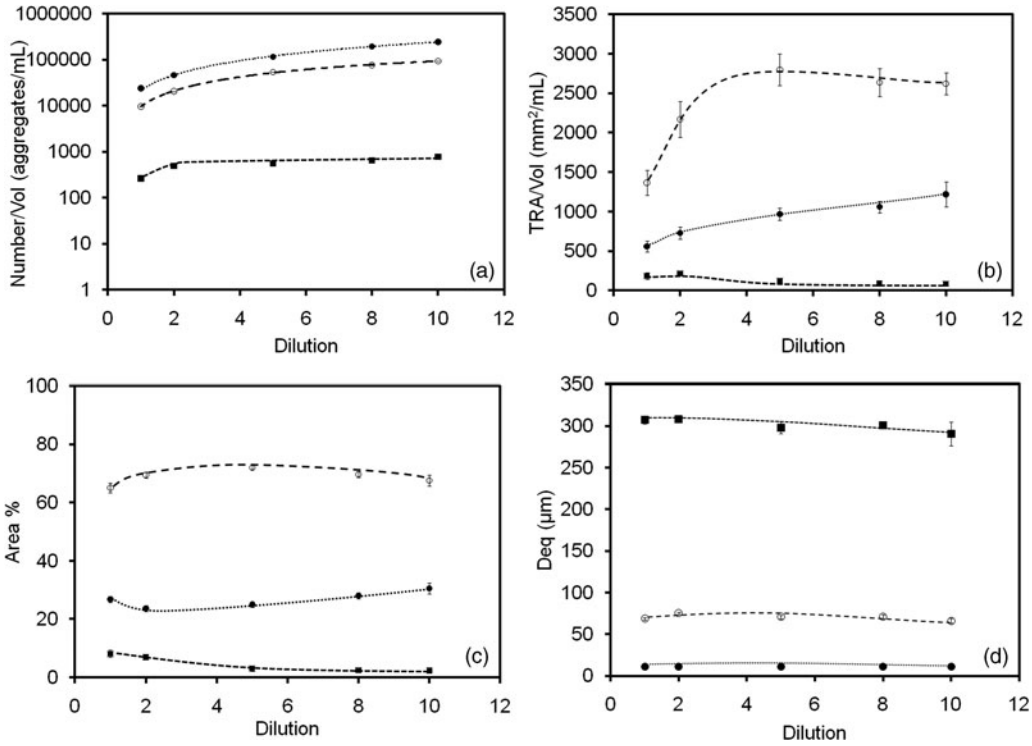

Figure 4. (**a**) Average number of aggregates per volume; (**b**) TRA/Vol, (**c**) average area percentage, (**d**) aggregates equivalent diameter for small (●), intermediate (○) and large (■) aggregates.

gates (Fig. 4b) demonstrates that from the twofold dilution onward there was an apparent decrease in the contents of those aggregates (run of four consecutive descending values), which could represent a deflocculating mechanism. With respect to the number of intermediate and small aggregates, both increased with dilution (*z-values* of 1.993 in both cases), pointing to either a deflocculating process or a disclosure of aggregates. Furthermore, until the tenfold dilution was performed, no asymptotic value was found; their numbers reached a value 10.19 times larger than the nondiluted sample for small aggregates, and 9.73 times larger for intermediate aggregates. Comparing these results with the TRA/Vol behavior (Fig. 4b), the twofold dilution caused the disclosure of enclosed aggregates, particularly of intermediate aggregates (marked increase from 1,366 to 2,169 mm^2/mL in the TRA/Vol of intermediate aggregates). From the twofold to the fivefold dilution, the increase of contents of intermediate (20,540 to 53,352 aggregates/mL and 2,169 to 2,798 mm^2/mL) and smaller (46,457 to 114,832 aggregates/mL and 729 to 969 mm^2/mL) aggregates behaved in the opposite manner to the larger aggregates (218 to 122 mm^2/mL). This suggests that there was some deflocculation of the larger aggregates (decrease in their contents), coupled with further disclosure of the intermediate and smaller aggregates (as shown by the overall increase of biomass content, from the twofold to the fivefold dilution; see Fig. 3a). Furthermore, there was a change in the driving force behind the aggregated biomass behavior from the fivefold dilution onward. There was deflocculation of the larger aggregates (and to some extent of the intermediate aggregates), as demonstrated by the decrease (run of three consecutive descending values) of the TRA/Vol values of the larger and intermediate aggregates until the tenfold dilution. The increase (run of three consecutive ascending values) of the contents of smaller aggregates (Fig. 4b) confirms this hypothesis. Except for the behavior of the number of intermediate and small aggregates throughout the dilution range, no *z-values* from the *runs test* were obtained to verify data randomness because there were too few data points (fewer than five) in the remaining cases.

The aggregates area percentage parameter (Fig. 4c) established the contribution of each aggregate class to the overall aggregated biomass. The increase of the intermediate area percentage after a twofold dilution (from 65.09% to 69.51%) was in opposition to the behavior of the smaller (26.84% to 23.61%) and larger aggregates (8.08% to 6.89%), and demonstrates the prevalence of the disclosure of these aggregates. With respect to the fivefold dilution, the significant decrease (6.89% to 3.00%) in the larger aggregates area percentage, and the increase in the intermediate (69.51% to 72.02%) and smaller (23.61% to 24.98%) aggregates, is consistent with an intermediate and smaller aggregates disclosure and a possible deflocculation of the larger aggregates. From the fivefold dilution onward, the small aggregates area percentage increased (run of three consecutive ascending values) while it decreased for the intermediate and

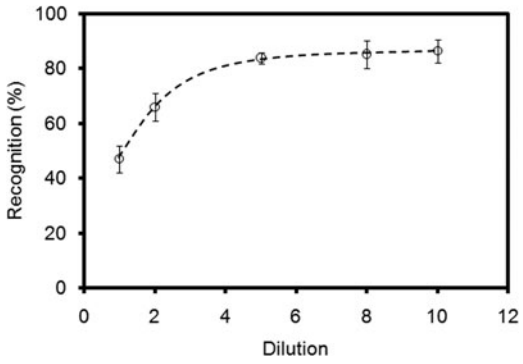

Figure 5. Aggregates recognition behavior for each dilution factor.

larger aggregates (runs of three consecutive descending values), consistent with the deflocculation of the intermediate and larger aggregates.

The behavior of the aggregates equivalent diameter (Fig. 4d) demonstrated that the small and intermediate aggregates remained stable with dilution (*z-values* of 0.6642 for both cases). However, the equivalent diameter of the larger aggregates decreased from the twofold dilution onwards (run of four consecutive descending values), indicating that deflocculation could have occurred.

To select the best dilution factor, the percentage aggregate recognition was determined and is presented in Figure 5 for each of the images acquired within each dilution.

The aggregates recognition percentage increased until the fivefold dilution (run of three consecutive ascending values), remaining fairly stable from this dilution onward, in agreement with the disclosure behavior of the small and intermediate aggregates (Fig. 5). The recognition percentage attained a maximum of approximately 80%, demonstrating an improved ability to separate enclosed and overlapping aggregates up to the fivefold dilution (increase of the aggregates recognition percentage). Furthermore, the 80% recognition percentage value may point to a maximum threshold for this parameter, considering the likelihood of aggregates being bisected by the image boundaries (implying recognition percentages below 100%) even at low magnification. Therefore, the recognition percentage parameter could be considered a valuable method for identifying the optimal dilution factor to assess aggregated biomass contents correctly.

Magnification Study

The effect of magnification on the determination of aggregates and protruding filamentous bacteria in the samples was determined. Given the poor pixel representation of any given aggregate under lower magnification, no morphological comparison, except for size, was performed between the two magnifications studied. As shown in Figure 2, the magnification change from 100× to 20× did not allow the aggregates contour to be recorded accurately, and no filamentous bacteria could be recognized.

As shown in Figure 6, a total of 13 samples, comprising both magnifications (approximately 25 images for each sample), were used to determine the number of aggregates per image and the aggregates number percentage, for sizes ranging from 0 to 200 μm (25 μm intervals).

Figure 6a demonstrates that more aggregates per image are obtained when images are acquired using 20× magnification. Therefore, it would be advantageous when working with higher magnifications such as 100× to increase the number of acquired images in order to increase the representativeness of the acquired data. In terms of the aggregates number percentage for each magnification, Figure 6b and Table 1 demonstrate an increase in the small aggregates for the 100× magnification; this would be expected given the size constraints of the 20× magnification for smaller aggregates. There were more large aggregates using the 20× magnification because of the size constraint of the 100× magnification for larger aggregates (Table 1).

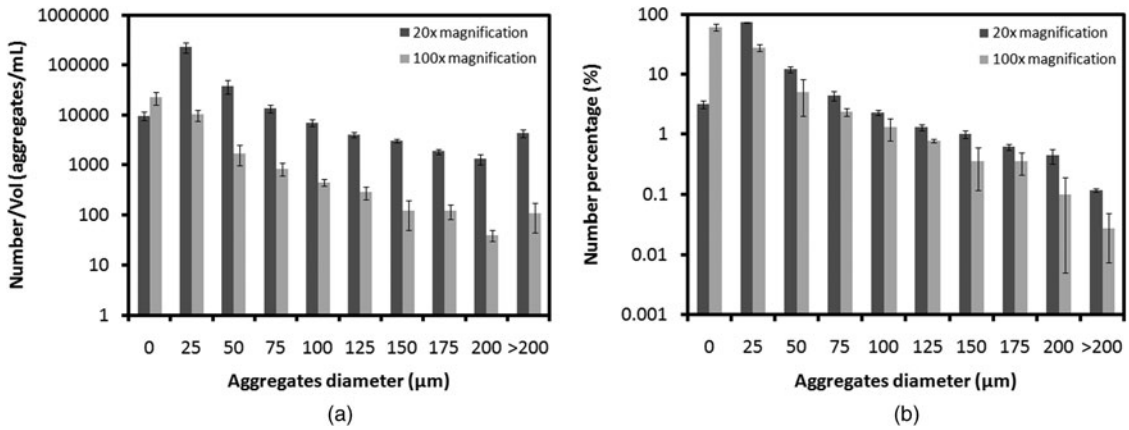

Figure 6. Histograms showing the behavior of aggregates based on size for 20× and 100× magnifications in (**a**) total number of aggregates per image and (**b**) aggregates number percentage.

Table 1. Aggregates Percentage for 20× and 100× Magnifications for the Small, Intermediate, and Large Aggregates.*

	Magnification	Small Aggregates (<0.025 mm)	Intermediate Aggregates (0.025–0.25 mm)	Large Aggregates (>0.25 mm)
Number %	20×	50.184 (4.466)	48.888 (4.397)	0.949 (0.303)
	100×	85.882 (3.257)	14.023 (3.250)	0.380 (0.168)
Area %	20×	24.108 (4.283)	67.702 (4.551)	8.357 (2.527)
	100×	55.874 (8.031)	42.616 (7.355)	4.299 (2.114)

*Standard deviations are presented in parentheses.

Table 2. *t*- and *p*-Values Obtained by the *t-Test Two Sample for Averages* ($\alpha = 0.05$) Regarding the Number and Area Aggregates Percentage for Small, Intermediate, and Large Aggregates, as Determined by the 20× and 100× Magnification Methodologies.

Variables	*t*-Value	*p*-Value
Small aggregates number %	26.594	2.450×10^{-12}
Intermediate aggregates number %	26.121	3.030×10^{-12}
Large aggregates number %	4.834	2.047×10^{-4}
Small aggregates area %	12.744	1.234×10^{-8}
Intermediate aggregates area %	8.444	1.077×10^{-6}
Large aggregates area %	5.517	6.634×10^{-5}

Table 2 presents the results of the *t*-test two-sample for averages (performed for an α-value of 0.05) in terms of the number and area percentages for the small, intermediate, and large aggregates, as determined by the 20× and 100× magnification methods. The number of observations was 13 in all cases, resulting in a Critical *t*-value of 1.782. As Table 2 demonstrates, the two methods led to different results as, in all cases, the *t*-value obtained surpassed the Critical *t*-value, and the *p*-value was always below 0.05. Therefore, the results presented in Tables 1 and 2 demonstrate that 20× magnification does not allow smaller aggregates to be identified accurately, whereas 100× magnification can lead to underestimation of larger aggregate contents. Therefore, in a scenario where large aggregates are present in representative numbers, a unique 100× magnification acquisition technique could entail some limitations.

To study the effect of magnification on the representativeness of overall biomass contents, the correlation of TRA/Vol between 20× and 100× magnification acquisitions was calculated and is presented in Figure 7; the average TRA/Vol and standard errors are presented in Table 3.

The results presented in Figure 7 reveal a good correlation (slope of 1.027) between the total aggregated biomass determined by the 100× and the 20× acquisition methods, although some dispersion was evident (correlation coefficient of 0.89). Furthermore, the average TRA/Vol values determined for the whole datasets (Table 3) demonstrated a high correlation between the two magnifications, resulting in an overestimation of 2.55% for the 100× magnification. In addition, the standard error obtained for the 100× magnification results was 36.7% lower than that for the 20× magnification, indicating that the 100× magnification acquisition method was more stable than the determination of aggregates contents. A two-sample *t*-test for averages (α-value of 0.05) was performed for the TRA/Vol parameter, as determined by the 20× and 100× magnification methods. The number of observations was 13, resulting in a Critical *t*-value of 1.782. Analyzing the *t*- and *p*-values obtained (0.591 and 0.283, respectively) demonstrates that the two methods gave similar results, as the *t*-value was lower than the Critical *t*-value and the *p*-value larger than 0.05. It may be concluded that the 100× magnification and

Table 3. Average TRA/Vol for the 20× and 100× Magnification Acquisitions and Corresponding Standard Deviations

	20× Magnification	100× Magnification	Error %
TRA/Vol ($mm^2/\mu L$)	9.845	10.067	2.55
Standard deviation	1.687	1.067	—

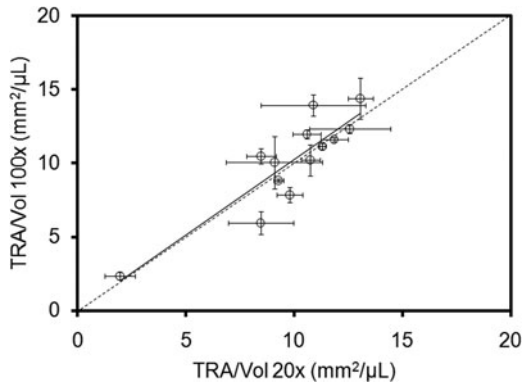

Figure 7. Correlation analysis of TRA/Vol between the 20× and 100× magnification acquisitions.

acquisition methodology allows both aggregates and filament data to be determined from the same slide, and smaller aggregates to be identified and characterized with no significant loss of accuracy regarding the representativeness of total biomass contents. However, when large aggregates are present in representative numbers, a complementary smaller magnification analysis would be advantageous.

Conclusions

This study demonstrated the vulnerability of image analysis to dilutions. We show that it is impossible to predict and quantify the dilution effect for the aggregated and filamentous biomass as a whole, on the basis of a single correction factor. It is also the case that when the assessment of biomass contents is not affected by further dilutions, this may not be true for the biomass structure. Therefore, the optimal operating dilution must be carefully established, and the determination of the aggregates recognition percentage could be a valuable methodology for identifying this dilution factor. For the image acquisition methodology, 100× magnification causes no loss in accuracy compared with the 20× magnification in terms of biomass representativeness and has the advantage of allowing aggregated and filamentous bacteria to be determined from a single image, and smaller aggregates to be identified and characterized.

Acknowledgments

The authors acknowledge financial support to D.P.M. and O.D. through the grant SFRH/BD/32329/2006 and the project POCI/AMB/57069/2004, respectively, provided by Fundação para a Ciência e Tecnologia (Portugal). The authors also express their gratitude to AGERE (Empresa de Águas, Efluentes e Resíduos de Braga – EM) and AGS (Administração e Gestão de Sistemas de Salubridade, S.A.) for their cooperation.

References

Abreu, A.A., Costa, J.C., Araya-Kroff, P., Ferreira, E.C. & Alves, M.M. (2007). Quantitative image analysis as a diagnostic tool for identifying structural changes during a revival process of anaerobic granular sludge. *Water Res* **41**, 1473–1480.

Amaral, A.L. (2003). Image analysis in biotechnological processes: Applications to wastewater treatment. PhD. Thesis. Braga, Portugal: University of Minho. Available at http://hdl.handle.net/1822/4506.

Amaral, A.L. & Ferreira, E.C. (2005). Activated sludge monitoring of a wastewater treatment plant using image analysis and partial least squares regression. *Anal Chim Acta* **544**, 246–253.

Amaral, A.L., Ginoris, Y.P., Nicolau, A., Coelho, M.A.Z. & Ferreira, E.C. (2008). Stalked protozoa identification by image analysis and multivariable statistical techniques. *Anal Bioanal Chem* **391**, 1321–1325.

Banadda, E.N., Smets, I.Y., Jenné, R. & Van Impe, J.F. (2005). Predicting the onset filamentous bulking in biological wastewater treatment systems exploiting image analysis information. *Bioproc Biosys Eng* **27**, 339–348.

Bradley, J.V. (1968). *Distribution-Free Statistical Tests*. Englewood Cliffs, NJ: Prentice-Hall.

Cenens, C., Van Beurden, K.P., Jenné, R. & Van Impe, J.F. (2002). On the development of a novel image analysis technique to distinguish between flocs and filaments in activated sludge images. *Water Sci Technol* **46**(1–2), 381–387.

Costa, J.C., Abreu, A.A., Ferreira, E.C. & Alves, M.M. (2007). Quantitative image analysis as a diagnostic tool for monitoring structural changes of anaerobic granular sludge during detergent shock loads. *Biotechnol Bioeng* **98**(1), 60–68.

da Motta, M., Amaral, A.L., Neves, L., Araya-Koff, P., Ferreira, E.C., Alves, M.M., Mota, M., Roche, N., Vivier, H. & Pons, M.N. (2002). Dilution effects on biomass characterization by image analysis. In *Proceedings of the 14th Brazilian Congress on Chemical Engineering*, Natal, Brazil, p. 9 (CD-ROM).

da Motta, M., Pons, M.N. & Roche, N. (2001). Automated monitoring of activated sludge in a pilot plant using image analysis. *Wat Sci Technol* **43**(7), 91–96.

Ginoris, Y.P., Amaral, A.L., Nicolau, A., Coelho, M.A.Z., Ferreira, E.C. (2007*a*). Recognition of protozoa and metazoa using image analysis tools, discriminant analysis, neural networks and decision trees. *Anal Chim Acta* **595**, 160–169.

Ginoris, Y.P., Amaral, A.L., Nicolau, A., Coelho, M.A.Z. & Ferreira, E.C. (2007*b*). Development of an image analysis procedure for identifying protozoa and metazoa typical of activated sludge system. *Water Res* **41**, 2581–2589.

Jenkins, D., Richard, M.G. & Daigger, G. (2003). *Manual on the Causes and Control of Activated Sludge Bulking, Foaming and Other Solids Separation Problems*. Boca Raton, FL: Lewis Publishing.

Jenné, R., Banadda, E.N., Gins, G., Deurinck, J., Smets, I.Y., Geeraerd, A.H. & Van Impe, J.F. (2006). Use of image analysis for sludge characterisation: Studying the relation between floc shape and sludge settleability. *Water Sci Technol* **54**(1), 167–174.

Jenné, R., Banadda, E.N., Smets, I.Y., Deurinck, J. & Van Impe, J.F. (2007). Detection of filamentous bulking problems: Developing an image analysis system for sludge composition monitoring. *Micros Microanal* **13**, 36–41.

Jin, B., Wilén, B.M. & Lant, P. (2003). A comprehensive insight into floc characteristics and their impact on compressibility and settleability of activated sludge. *Chem Eng J* **95**, 221–234.

Mesquita, D.P., Dias, O., Amaral, A.L. & Ferreira, E.C. (2009*b*). Monitoring of activated sludge settling ability through image analysis: Validation on full-scale wastewater treatment plants. *Bioprocess Biosyst Eng* **32**(3), 361–367.

Mesquita, D.P., Dias, O., Amaral, A.L. & Ferreira, E.C. (2010). A Comparison between bright field and phase-contrast image analysis techniques in activated sludge morphological characterization. *Micros Microanal* **16**(2), 166–174.

Mesquita, D.P., Dias, O., Dias, A.M.A., Amaral, A.L. & Ferreira, E.C. (2009*a*). Correlation between sludge settling ability and image analysis information using partial least squares. *Anal Chim Acta* **642**(1–2), 94–101.

Wilén, B.M., Lumley, D., Mattsson, A. & Mino, T. (2008). Relationship between floc composition and flocculation and settling properties studied at a full scale activated sludge plant. *Water Res* **42**, 4404–4418.